Proceedings of the 1993 IEEE/RSJ International Conference on Intelligent Robots and Systems Yokohama, Japan July 26-30, 1993

Fast Path Planning Available for Moving Obstacle Avoidance by Use of Laplace Potential

Sadao AKISHITA
Takashi HISANOBU and Sadao KAWAMURA

Dept. of Mechanical Engineering, Ritsumeikan University
Kita-ku, Kyoto 603-77, JAPAN

ABSTRACT

This work describes the theory and the experiment of a fast path planning available for moving obstacle avoidance for an autonomous mobile robot by use of Laplace potential. This new navigation function for the path planning is feasible to guide on real time a mobile robot avoiding arbitrarily moving obstacles and reaching the goal. The experiment is conducted to verify the effectiveness of the navigation function in the obstacle avoidance in the real world. The experimental systems are composed of a position sensing camera, a mobile robot and a computer for processing the position signal and for controlling the velocity vector of the robot. Three examples of the experiment are presented; first the avoidance from a standing obstacle, secondly the avoidance from a moving obstacle in parallel lines-bounded space and thirdly the avoidance from one moving obstacle and another standing obstacle. The robot can reach the goal after successfully avoiding the obstacles in all cases.

1. INTRODUCTION

An autonomous path planning increases its demand for many industrial field such as nuclear power plant and vehicle automation in warehouse. Two approaches for planning the path have been investigated; Artificial Intelligince (AI) approach and physical field approach such as mechanical potential function. When the information of the environment is ambiguous, only AI approach is feasible. Recently efficient image processing systems become available and hence geometric information of the robot and obstacles in given environment can be accessible. Physical field approach is more attractive than AI approach for its high efficiency in the path planning. Artificial potential functions have been proposed and investigated since Takegaki[1)] and Khatib[2)]. A mobile robot applys the force generated by the artificial potentials as control input to the driving systems. Modified potentials have been devised to overcome the dead point of the null resultant force[3)]. The more generic potential function free from the local minimum is proposed by Koditschek[4,5)]. The authors proposed a new navigation function utilizing hydrodynamic potential applicable for guiding a mobile robot which can avoid a moving obstacle and can reach the goal[6,7)]*. The essential point of the idea is that the dynamics of the water flow is applicable to generate the navigation function. The work space for the robot is compared to the flow field, such as the goal to the flow sink and the obstacle to the closed boundary of the doublet. The path for the robot corresponds to the stream line.

The flow is described with velocity potential function, a kind of Laplace potential. The complex function theory is applied to represent the two-dimensional flow itself. The conformal mapping theory is introduced to describe an arbitrary boundary shape of the obstacle in the work space for the robot. The hydrodynamic potential is compatible with unsteady boundary condition. This means that the path for the robot to avoid the moving obstacle is calculated with the hydrodynamic potential within so reasonable time that it can be applicable to the real time path planning. Another advantage brought to this approach is that a unique solution is guaranteed for the path planning, for any rule is not utilized. This fact becomes very important for the case of avoidance from multi moving obstacles. In order to maintain this advantage we persistently utilize the dynamics of fluid flow as shown below.

The first objective of this paper is to discuss the applicability of our new navigation function in the real world. Since the applicability to a still obstacle is self-evident, the discussion is focussed on a moving obstacle. After a basic formulation where a circle-shaped moving obstacle is modelled as a doublet is presented, the practical condition resulted from the finite sample time in the real world is investigated. A new navigation function feasible to two moving obstacles is then introduced, by which a mobile robot can reach the goal avoiding two arbitrarily moving obstacles. The second objective of this paper is to verify the effectiveness of the navigation function in the real world. The experiment to realize the objective is conducted in the frame of the geometric information acquired by an optical image device. The velocity command for the robot on the path is computed by a personal computer. A sample time interval should be short enough for the robot to avoid an obstacle with considerable approaching speed. The feasibility of the robot and control system including the optical measuring device is proved by the experiment.

*The author found the paper proposing a hydrodynamic potential for obstacle avoidance by D.Megherbi and W.A.Volovich in Proceedings of the IEEE International Conference on Robotics and Automation, 1992. But the author should claim the priority of his paper as the publication of the papers[6)] is clearly earlier than the above mentioned paper

0-7803-0823-9/93/$3.00 (C) 1993 IEEE

2. NAVIGATION FUNCTION

As the mathematical construction of the new navigation function is dropped in this paper, the reader should refer to the author's previous paper[6]. The navigation function is briefly described in the following.

We assume that the motion control system of a mobile robot is represented as follows in two dimensional field,

$$\begin{cases} \dot{x}_p &= u \\ \dot{y}_p &= v \end{cases} \tag{1}$$

where (x_p, y_p) represents the center point of the robot, and $(u, v)^T$ represents the velociy control command to the system. As the input $(u, v)^T$ is generated by applying hydrodynamic potential, it is convenient to introduce complex variables into the expression of u and v,

$$u + iv \;=\; K(r)w_s + w_a \tag{2}$$

where w_s and w_a are the hydrodynamic complex velocities, the former of which is applied for the robot to reach the goal, and the latter of which is applied for the robot to avoid a moving obstacle. $K(r)$ is the function of r that means the distance between the point $(x_p + iy_p)$ and the goal, and it is introduced for modifying the hydrodynamic complex velocity w_s so that the robot may stop smoothly at the goal. w_s is represented by a sink on the goal point z_s,

$$\bar{w}_s \;=\; \frac{-m}{z_p - z_s}, \quad (z_p \;=\; x_p + iy_p) \tag{3}$$

where m means the sink strength. Since the magnitude of $\bar{w}_s$ increases to infinity as the robot approaches the goal $(z_p \to z_s)$, the robot cannot stop smoothly at the goal. Then $K(r)$ must relax the abrupt increase by the function of r,

$$K(r) \;=\; \left(\frac{r}{R}\right)\left[1 - e^{(-c_1 r)}\right] \tag{4}$$

where R is the radius of the circle representing an obstacle and c_1 is relevant positive factor.

2.1. Single moving obstacle in free space

When the boundary of an obstacle is represented by the equation,

$$G(x, y; t) \;=\; 0 \tag{5}$$

the boundary condition on the obstacle surface is,

$$\frac{\partial G}{\partial t} + u_a\frac{\partial G}{\partial x} + v_a\frac{\partial G}{\partial y} \;=\; 0 \;\;;\;\; \text{on the boundary} \tag{6}$$

where w_a in Eq.(2) is represented as $w_a = u_a + iv_a$.
For a still obstacle the boundary condition Eq.(6) allocates the flow velocity along the tangential direction on the boundary. We assume a circle of radius R as the simplest and typical obstacle shape. The hydrodynamic velocity expression for a still circle is represented by,

$$\bar{w}_s \;=\; -m\left(\frac{1}{z_p - z_s} + \frac{1}{z_p - z_s'} - \frac{1}{z_p - z_0}\right) \tag{7}$$

where z_0 means the location of the center of the obstacle and z_s' is the position of the imaginative sink inside the circle. The position z_s' is determined by the following equation related with the center point z_0 and the sink position z_s,

$$(z_s - z_0)(\bar{z}_s' - \bar{z}_0) \;=\; R^2 \tag{8}$$

For a moving obstacle the boundary condition Eq.(6) allocates the flow velocity along the direction of the surface element velocity on the boundary. In the case of circle-shaped obstacle this is represented by a doublet as shown in Eq.(9),

$$\bar{w}_a \;=\; \frac{RUe^{i\alpha}}{(z - z_0)^2} \tag{9}$$

where $Ue^{i\alpha}$ means the translational velocity of the center of the moving obstacle. The velocity thus induced represents the moving effect of the obstacle. The total navigation function for a single moving obstacle is constructed by Eq.(7) that represents the instantaneously standing obstacle effect and also by Eq.(9) that represents the moving obstacle effect considering the modification represented by Eq.(2),

$$u - iv \;=\; -K(r)m\left(\frac{1}{z_p - z_s} + \frac{1}{z_p - z_s'} - \frac{1}{z_p - z_0}\right) + \frac{R^2 Ue^{i\alpha}}{(z - z_0)^2} \tag{10}$$

Now we assume the radius R as the sum of the radius of the robot circle a_r and the radius of the obstacle circle a_0,

$$R \;=\; a_r + a_0 \tag{11}$$

Then the motion control algorithm, Eq.(1), is applied on the center of the robot. As the robot has no volume and then no mass in this algorithm, the robot can obey any velocity command. Even if the velocity command is not realized, the robot can find anytime and anywhere a renewed path which can lead to the goal. This path does not cause any crash on the obstacle or on the boundary, if the radius a_r is added to the normal distance on the surface of the obstacle as shown in Eq.(11) or on the boundary. In case of a moving obstacle we should put the assumption that a moving robot with radius R cannot sit on the goal point anytime. When this assumption is broken, the path leading to the goal cannot be found.

2.2 Single moving obstacle in bounded space

The navigation function for single moving obstacle in bounded space is acquired by applying conformal mapping to adjust the flow velocity on the boundary. Actually to find an appropriate mapping function is not always easy. The mapping function by which two parallel lines are transformed to a typical shape is rather simple[7]. Then the authors obtained the flow velocity function $\bar{w}(z_p)$ for the robot that should avoid an obatacle and reach the goal in a bounded space between parallel linear walls at $z = \pm ih$ as shown in Fig.1. $\bar{w}(z_p)$ is composed of three parts.

$$\bar{w}(z_p) \;=\; \bar{w}(z_p)_d + \bar{w}(z_p)_s + \bar{w}(z_p)_m \tag{12}$$

First term $\bar{w}(z_p)_d$ represents direct effect of a doublet.

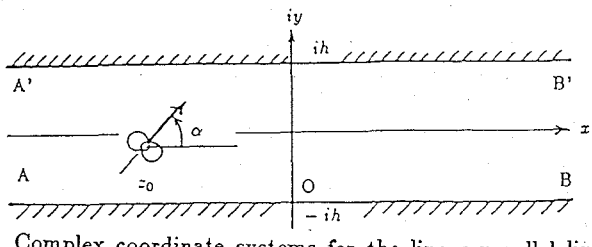

Fig.1 Complex coordinate systems for the linear parallel lines boundary

$$\bar{w}(z_p)_d = \left(\frac{-i\mu\pi\exp(-i\beta)}{8h}\right)\left\{[1+\coth\varpi(z_p-z_0)]^2 - \frac{\exp[\varpi(z_p-\bar{z}_0)]}{\cosh[\varpi(z_p-z_0)]}(1+\tanh[\varpi(z_p\bar{z}_0)])\right\} \quad (13)$$

where $\varpi = \pi/4h$, and μ and β should satisfy the following relation with U, R and α.

$$\mu = \frac{\pi UR}{h}\exp(2\varpi x_0), \quad \beta = \frac{\pi}{2}+\alpha+2\varpi y_0 \quad (14)$$

The second term $\bar{w}(z_p)_s$ represents the direct effect of a sink.

$$\bar{w}(z_p)_s = (2\varpi m)\left\{\frac{2\exp(4\varpi z_p)-E_{ps}+E_{p\bar{s}}}{E_{s\bar{s}}+E_{ps}+E_{p\bar{s}}}\right\} \quad (15)$$

$$E_{ps} = \exp[2\varpi(z_p+z_s)], \quad E_{p\bar{s}} = \exp[2\varpi(z_p+\bar{z}_s)],$$

$$E_{s\bar{s}} = \exp[2\varpi(z_s+\bar{z}_s)]$$

The third term $\bar{w}(z_p)_m$ represents the imaginative effect of the sink at z_s' and z_0.

$$\bar{w}(z_p)_m = (2\varpi m)\left\{\frac{2\exp(4\varpi z_p)-E_{ps'}-E_{p\bar{s}'}}{E_{s'\bar{s}'}-\exp(4\varpi z_p)+E_{ps'}-E_{p\bar{s}'}} - \frac{2\exp(4\varpi z_p)-E_{po}-E_{p\bar{o}}}{E_{o\bar{o}}-\exp(4\varpi z_p)+E_{po}-E_{p\bar{o}}}\right\} \quad (16)$$

$$E_{ps'} = \exp[2\varpi(z_p+z_s')], \quad E_{p\bar{s}'} = \exp[2\varpi(z_p+\bar{z}'_s)],$$

$$E_{s'\bar{s}'} = \exp[2\varpi(z_s'+\bar{z}'_s)], \quad E_{po} = \exp[2\varpi(z_p+\bar{z}_0)],$$

$$E_{p\bar{o}} = \exp[2\varpi(z_p+z_0)], \quad E_{o\bar{o}} = \exp[2\varpi(z_0+\bar{z}_0)]$$

2.3 Two moving obstacles in free space

For the case of multi-moving obstacles the acquistion of the flow function is rather complicated. Although the acquisition of the mapping function compatible to the condition on the boundary is ascertained, but its actual acquisition is not easy. One of expedients by which this difficulty is circumvented is to introduce "a rule ". Suppose that a mobile robot must avoid two moving obstacles on the way to the goal. The robot concentrates on avoidance from the closest obstacle at first and forget another obstacle. After first avoidance is successful, then the robot concentrates on the second avoidance. The navigation function is simple in applying this kind of expedient. But an appropriate switching from the first avoidance to the second avoidance is not always assured. When the switching is delayed (this is always possible as long as a rule is applied), can the robot avoid from the second obstacle always? The authors insist on utilizing the physics of the field. A new navigation function for two moving obstacles are introduced in the following.

Suppose that two moving circular obstacles C_1 and C_2 with the velocities, $U_1e^{i\alpha_1}$ and $U_2e^{i\alpha_2}$, locate on z_1 and z_2 respectively, while the goal position is z_s. The flow velocity function for each of two moving obstacles when the mutual interactive effect is neglected,

$$\bar{w}_1(z) = \bar{w}_{s_1}+\bar{w}_{d_1} \quad (17)$$

$$\bar{w}_{s_1}(z) = -\left(\frac{m}{z-z_s}+\frac{m}{z-z_{s_1}}-\frac{m}{z-z_2}\right), \quad \bar{w}_{d_1}(z) = -\frac{a_1^2U_1e^{i\alpha_1}}{(z-z_1)^2}$$

$$\bar{w}_2(z) = \bar{w}_{s_2}+\bar{w}_{d_2} \quad (18)$$

$$\bar{w}_{s_2}(z) = -\left(\frac{m}{z-z_s}+\frac{m}{z-z_{s_2}}-\frac{m}{z-z_2}\right), \quad \bar{w}_{d_2}(z) = -\frac{a_2^2U_2e^{i\alpha_2}}{(z-z_2)^2}$$

where a_1 and a_2 are the radius of the circle C_1 and C_2 respectively. z_{s_1} and z_{s_2} mean the position of the imaginative sink induced by the sink on the goal z_s inside the circle C_1 and C_2 respectively. z_{s_1} and z_{s_2} must satisfy the following equations respectively,

$$(z_s-z_1)(\bar{z}_{s_1}-\bar{z}_1) = a_1^2 \quad (19)$$

$$(z_s-z_2)(\bar{z}_{s_2}-\bar{z}_2) = a_2^2 \quad (20)$$

Considering the imaginative doublet inside the circle by the external doublet, $\bar{w}_{d_1}$ and $\bar{w}_{d_2}$ are corrected as follows,

$$\bar{w}_{d_1}(z) = -\frac{a_1U_1^2e^{i\alpha_1}}{(z-z_1)^2}+\frac{a_2^2U_2(a_1/l)^2e^{i(2\varphi-\alpha_2)}}{(z-z_1')^2}-\frac{a_2^2U_2e^{i\alpha_2}}{(z-z_2)^2} \quad (21)$$

$$\bar{w}_{d_2}(z) = -\frac{a_2U_2^2e^{i\alpha_2}}{(z-z_2)^2}+\frac{a_2^2U_1(a_2/l)^2e^{i(2\varphi-\alpha_1)}}{(z-z_2')^2}-\frac{a_1^2U_1e^{i\alpha_1}}{(z-z_1)^2} \quad (22)$$

noindent where z_1' and z_2' are the positions of the imaginative doublet satisfying the following equations,

$$(z_1-z_2)(\bar{z}_1-\bar{z}'_1) = a_1^2 \quad (23)$$

$$(z_2-z_1)(\bar{z}_2-\bar{z}'_2) = a_2^2 \quad (24)$$

l is the distance between the center positions of the two circles and φ is the argumental angle of z_2-z_1,

$$z_2-z_1 = le^{i\varphi} \quad (25)$$

The corrected flow velocity functions $\bar{w}_1(z)$, $\bar{w}_2(z)$ satisfy the boundary condition on the circle boundary C_1 and C_2 respectively. Then the following function $\bar{w}(z)$ not only satisfies the boundary condition on two point Q_1 and Q_2 as shown in Fig.2,

$$\bar{w}(z) = (1-\alpha)\bar{w}_1+\alpha\bar{w}_2, \quad \alpha = \frac{|z-(a_1e^{i\varphi}+z_1)|}{l-a_1-a_2} \quad (26)$$

but also $\bar{w}(z)$ is appropriate on the line between Q_1 and Q_2. This idea can be expanded to whole field. Suppose that the robot center position locates on $P(z=z_p)$ as shown in Fig.2, then the velocity command is given by

$$u-iv = -K(r)\{(1-\alpha)w_{s_1}(z_p)+\alpha w_{s_2}(z_p)\} + (1-\alpha)w_{d_1}(z_p)+\alpha w_{d_2}(z_p) \quad (27)$$

$$\alpha = \frac{r_1}{r_1+r_2}, \quad r_1 = |z_p-z_1|-a_1, \quad r_2 = |z_p-z_2|-a_2 \quad (28)$$

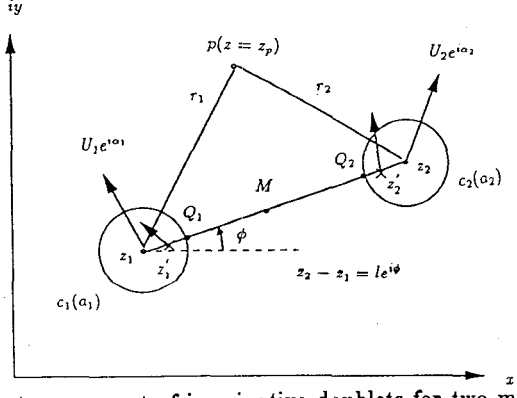

Fig.2 Arrangement of imaginative doublets for two moving obstacles

3. REMARKS ON PRACTICAL USE

The control of a mobile robot locomotion is actually executed by using a computer. Therefore discrete time control is applied in the real world. This means that we should overcome the error arising from the model difference. The geometric data of the robot and the obstacle are obtained by processing the data of vision signal. The control command is fed from the computer by processing the geometric data. The time delay necessary for processing the data is inevitable to the control system. The control command described by Eq.(1) is derived on the assumption that the data are processed with no time delay. An example exhibiting the fail of avoidance from a moving obstacle is shown in Fig.3(a). In this case the total time delay is $\Delta t = 0.6$sec, for the speed of the obstacle; $U_0 = 14.1$cm/sec. The mobile robot fails in avoiding the obstacle, then the robot hits the obstacle. One of measures by which the robot circumvents crashing is to redefine the radius of the obstacle. Now, the total time delay is defined as Δt, and the maximum approaching speed is defined as U_a. Then the redifined radius of the obstacle R should be increased from the original radius R_o by $U_a \Delta t$ at least as follows,

$$R > R_o + U_a \Delta t \tag{29}$$

Since R is longer at least by the maximum approaching distance in Δt than the actual radius R_o, the robot cannot approach the obstacle inside the inhibited zone. Fig.3(b) shows an example of the successful avoidance where R is increased by $0.1R_0$ than the original radius adopted Fig.3(a).

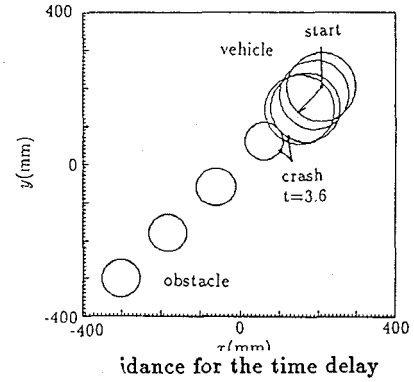

idance for the time delay

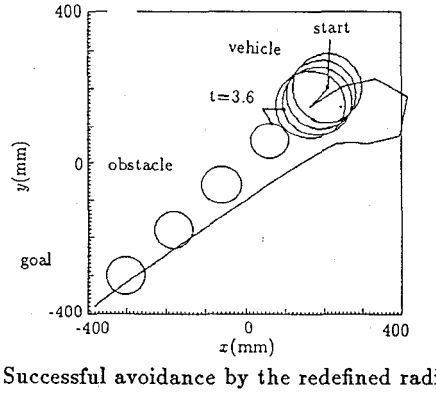

(b) Successful avoidance by the redefined radius

Fig.3 Effect of extended avoidance radius

4. EXPERIMENT

Figure 4 shows the schematics of experimental systems. Infra-red Light Emitting Diodes (LEDs) are installed on the top of the robot and also on the top of the obstacle. Position Sensing Device (PSD) can obtain a bird's eye view of the robot and the obstacle by sensing the infra-red light emitted from LEDs. As PSD can access only single point at a time, the plural spots of LED are detected by utilizing time division technique. Acquisition of the position of a LED is sychronized with emission of infra-red light from the LED. This sequence is controlled by PSD controller. The locations of the robot and the obstacle are identified by PC-9801DA computer. The control command to the robot is fed by wire from the PC computer. The robot is drived by two pulse motors each of which controls each velocity of the two wheels independently as shown by,

$$v_{left} = v - K_c \frac{l_w \Delta\theta}{2T}, \quad v_{right} = v + K_c \frac{l_w \Delta\theta}{2T} \tag{30}$$

where v_{left} and v_{right} are the speed of the left wheel and that of the right wheel respectively, v is the speed command of the center of the robot, $\Delta\theta$ is the steering command, l_w is the distance between the two wheels, T is the sample time of the system and K_c is the suitable gain for steering control. Figure 5 shows the control block diagram of the total systems.PCL-80K is a digital processor board where the velocity command to the driving motor is converted to the corresponding pulse signal.

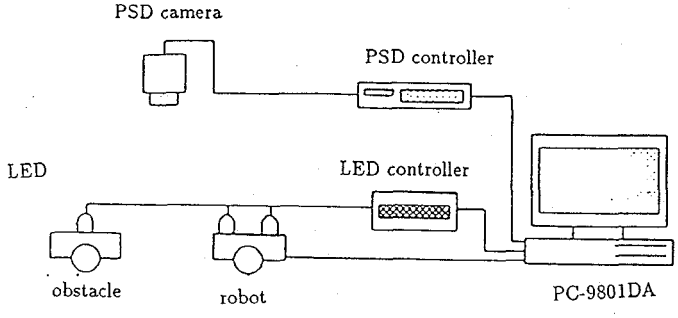

Fig.4 Experimental systems

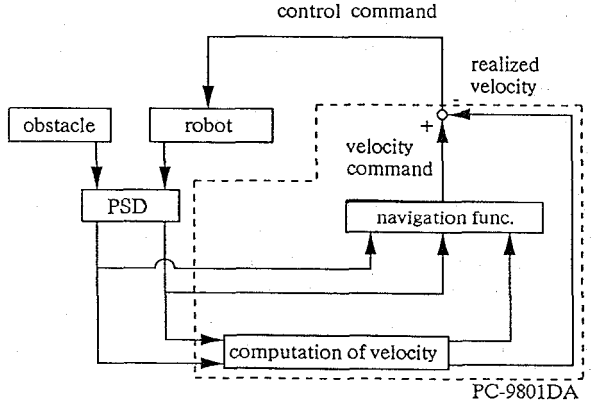

Fig.5 Block diagram of control experimental systems

4.1 Avoidance from stationary obstacle

First one of experimental results is presented for a stationary obstacle. The radius of the obstacle R is determined as $R = a_0 + a_r = 14\text{cm}$ (a_r : radius of robot). The sample time of the total system T is 17 msec. The distance l_w is 10.8 cm. These values are fixed throughout the experiment. Figure 6(c) shows two trajectories of the robot; thin line as command path and solid line as realized path. These two lines agree rather well. The difference between the two increases as the steering command increases. Figure 6(a) and 6(b) show the velocity-time history of the robot and the azimuth-time history of the robot respectively. Time delay of about 0.5 sec is found between the command curve and the realized curve. The time delay is caused from filtering the signal with cut-off frequency of 1 Hz. The trajectory is successful in spite of the time delay.

4.2 Avoidance from single moving obstacle in bounded space

Secondly the other result of experiment is presented for a moving obstacle in parallel lines boundary. The breadth between two lines is $40cm$, where an approach and avoidance of the autonomous robot is simulated for another moving vehicle in straight lane. Figure 7(a)~(c) shows the result of the experiment. The reader can understand from Fig.7(c) that the robot meets an obstacle moving head-on in a lane and that the robot finally reaches the goal after avoiding the obstacle. The sample time of the total system T is 20 msec only a little larger than the above mentioned time, although the volume of path planning calculation increases remarkably as shown by Eq.(12)~(16). The speed of the moving obstacle was 5.6 cm/sec constantly while that of the robot is rather higher as found from Fig.7(c), Figures 7(a) and (b) show the velocity-time history and the azimuth-time history of the robot respectively. The trajectory is successful although the time delay is found between the calculations of guidance velocity and azimuth angle and the experimental results of those.

4.3 Avoidance from two obstacles in free space

The third examples are avoidances from two obstacles. Figures 8 (a), (b) and (c) represent the experimental result where the robot avoids one moving obstacle and then the other standing obstacle. As shown in Fig.8 (a), the robot avoids the first obstacle on rear side. Hence we can find the dragged flow effect by the obstacle motion on the earlier part of the trajectory. Figures 8 (b) and (c) show the velocity-time history of the robot and the azimuth-time history of the robot respectively. The differences between the planned value and the realized value in (b) and (c) are not small. But the trajectory is successful in this case.

Figures 9 (a),(b) and (c) show an experimental result by which the robot can avoid the two moving obstacles one after another then can reach the goal. In this case the robot avoids each obstacle on their front. The trajectory of the robot is very smooth, but it is not a globally optimal way, as it is determined temporarily by the local condition.

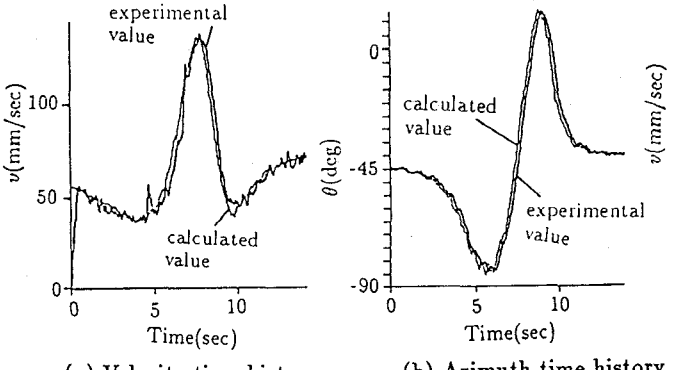

(a) Velocity-time history (b) Azimuth-time history

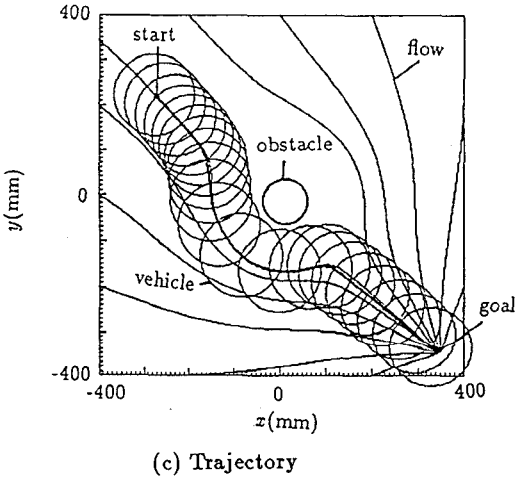

(c) Trajectory

Fig.6 Approach and avoidance from a standing obstacle

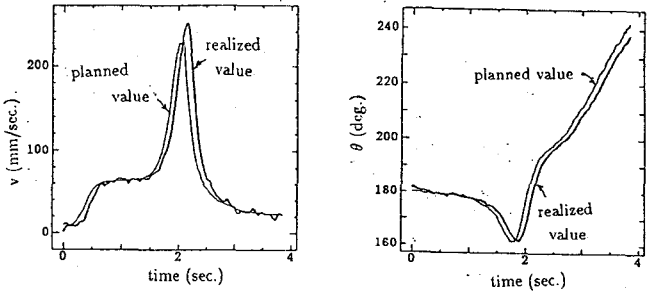

(a) Velocity-time history (b) Azimuth-time history

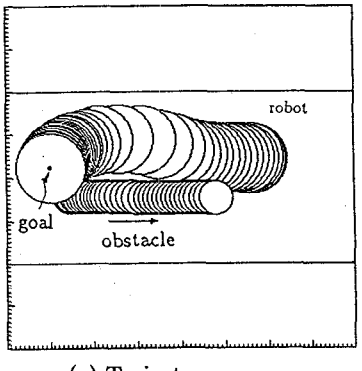

(c) Trajectory

Fig.7 Approach and avoidance from a moving obstacle in parallel lines boundary

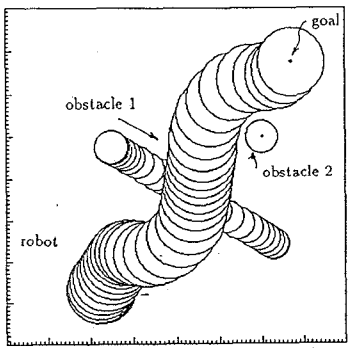

(a) Final path trajectory

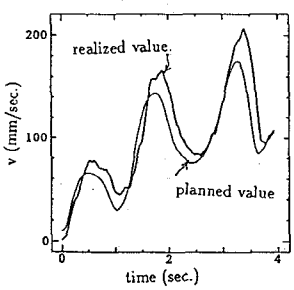

(b) Velocity-time history

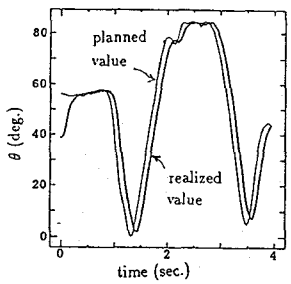

(c) Azimuth-time history

Fig.8 Approach and avoidance from one moving obstacle and another standing obstacle

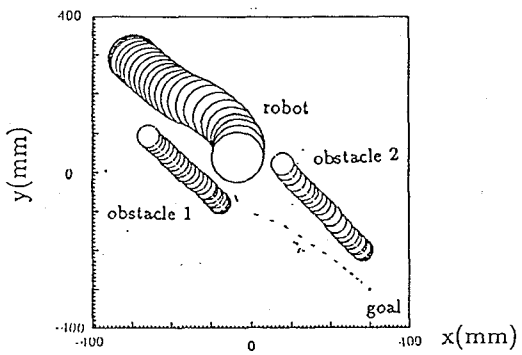

(a)Intermediate path trajectory

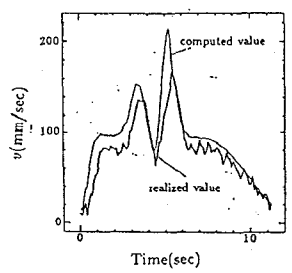

(b) Velocity-time history

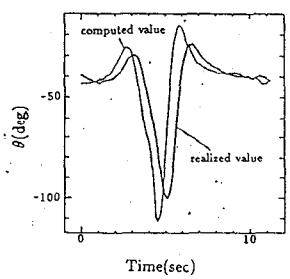

(c) Azimuth-time history

Fig.9 Approach and avoidance from two moving obstacles

5. CONCLUDING REMARKS

A new navigation function for the path planning available for moving obstacle avoidance was introduced. This new navigation function is feasible to guide on real time a mobile robot avoiding even two moving obstacles in free space. The experiment was conducted successfully for the case of two moving obstacles in free space and a single moving obstacle in bounded space. This result proved the effectiveness of the new navigation function in the real world. The path planning algorithm is feasible to the real-time guidance for an autonomous mobile robot. Actually if a high speed custom-made computer is introduced into the guidance systems, the real time planning for the practical robot can be realized.

REFERENCE

1. M.Takegaki and S.Arimoto, "A New Feedback Method for Dynamic Control of Manipulators ", Trans. ASME, J. of Dynamic Systems, Measurement and Control, Vol.103, pp.119, 1982.
2. O.Khatib, "Real-time obstacle avoidance for mainipulators and mobile robots ", Int. J. for Robotics Research, Vol.5, NO.1, pp.90-98, 1986.
3. P.Khosla and R.Volpe, "Superquadric potential for obstacle avoidance and approach ", Proc. IEEE Conference on Robotics and Automation, Philadelphia, 1988, pp.1778-1784.
4. D.E.Koditschek, "The control of natural motion in mechanical system ", Trans. of ASME Journal of Dynamic Systems, Measurement and Control, Vol.113, Dec.1991, pp.547-551.
5. D.E.Koditschek, "Some application of natural motion control ", Trans. of ASME Journal of Dynamic Systems, Measurement and Control, Vol.113, Dec.1991, pp.552-557.
6. S.Akishita, S.Kawamura and K.Hayashi, "New Navigation Function Utilizing Hydrodynamic Potential for Mobile Robot ", Proc. of the IEEE International Workship on Intelligent Motion Control, Bogazici University, Istanbul, Turkey, 1990, pp.413-417.
7. S.Akishita, S.Kawamura and T.Hisanobu, "Velocity Potential Approach for Path Planning to Avoid Moving Obstacles", to appear at Journal of Advanced Robotics, 1993.